Supporting Information

Appropriate Zn^{2+}/Mn^{2+} concentration of the electrolyte enables superior performance of AZIBs

Qihang Dai[1], Longyan Li[1]*,, Tiancheng Tu[1] Mingdao Zhang[2], Li Song[2]

[1]School of Chemistry and Materials Science, Nanjing University of Information Science and Technology, Nanjing 210044, China

[2]School of Environmental Science and Engineering, Nanjing University of Information Science and Technology, Nanjing 210044, China

*Corresponding author.

E-mail addresses: lilongyan@nuist.edu.cn (Longyan Li).

Experimental section

Preparation of MnO and β-MnO_2

4g $KMnO_4$ was dissolved in 200 mL of 2.5 mol/L H_2SO_4 and stirred at 75 °C for 2 h. The precipitate was centrifuged and rinsed thoroughly with deionized water and then dried at 60 °C for 12 h, and the brown powder was calcined at 400 °C for 10 h under H_2/Ar environment to obtain MnO.

2.1 mmol of $(NH_4)_2SO_4$ and 2.1 mmol of $MnSO_4$ were dissolved in 30 mL of deionized water. The above solution was transferred into two 100 mL Teflon-lined autoclaves. Then, the Teflon-lined autoclaves were put in a constant temperature oven that was kept at 120 ℃ for 12 h. The production was filtered, rinsed thoroughly with deionized water, and then dried at 60 °C for 12 h to obtain *β*-MnO_2.

Preparation of electrolytes

$ZnSO_4$ and $MnSO_4$ were dissolved directly in deionized water to prepare 2 M $ZnSO_4$, 2 M $ZnSO_4$ + 0.1 M $MnSO_4$, 2 M $ZnSO_4$ + 0.5 M $MnSO_4$, 2 M $ZnSO_4$ + 0.8 M $MnSO_4$, 0.5 M $MnSO_4$, 0.1 M $ZnSO_4$ + 0.1 M $MnSO_4$, 0.5 M $ZnSO_4$ + 0.5 M $MnSO_4$, and 0.1 M $ZnSO_4$ + 0.8 M $MnSO_4$ electrolytes.

All the chemicals were analytical reagent and purchased from Aladdin Industrial Co., Ltd. (China).

Structural characterizations

Phase identification of all the samples was performed by X-ray diffraction (XRD) (Rigaku Co, Cu Kα 1.5406A, 40 kV 40 mA, D/teX Ultra 250 detector). A scanning electron microscope (SEM) was used to observe the morphology of these samples. X-ray photoelectron spectroscopy (XPS) (Thermo Scientific K-Alpha) was used to determine the chemical state of the cathode. The amount of manganese in the electrolyte after a certain number of cycles was measured by inductively coupled plasma optical emission spectrometry (ICP-OES) (Thermo Fisher ICAP PRO).

Electrochemical tests

LIR-2032 coin-type cells assembled in ambient air were used to measure the electrochemical performance of all the samples. The active materials, conductive agent (acetylene black), and binder (PVDF) were thoroughly mixed with a weight ratio of

7:2:1 in N-methyl-2-pyrrolidone (NMP) solvent. Then, the obtained slurry was applied to a carbon paper and dried at 60 ℃ for 12 h in a vacuum oven, respectively. The mass loading of the cathode material was about 0.8 mg cm^{-2}. The zinc foil was used as the anode. The aqueous electrolytes were those 8 solutions described previously. The galvanostatic charge-discharge and the galvanostatic intermittent titration technique (GITT) test of the coin cells were operated between 1.0 and 1.85 V *vs*. Zn^{2+}/Zn at room temperature on a NEWARE battery tester (NEWARE Battery Test System, Neware Co. Ltd., China). CV and EIS test of batteries were carried out on the Chi 660e electrochemical workstation (CH Instruments Inc).

Calculation 1: Cell capacity contribution

The ratio of capacitive contribution to the total capacity can be qualitatively analyzed according to the formula below:[1]

$$i = av^b \quad (1)$$

Herein, i and v represent peak currents (mA) and scan rates (mV s^{-1}), respectively. a and b represent adjustable parameters. According to previous reports, the b value reveals ion kinetic information based on the battery system. A b value of 0.5 is representative of diffusion-controlled behavior, while a b value of 1 is indicative of ideal capacitive-controlled behavior.[2]

Calculation 2: Calculation of Zn^{2+} diffusion coefficient (D_{Zn}^{2+}) by the galvanostatic intermittent titration technique (GITT)

In the GITT measurement, the cells were charged/discharged for 40 min, and then relaxed for 30 min to let the voltage reached equilibrium. The process was repeated until the voltage reached 1.85 V and 1 V for 2 cycles.

As shown in Fig. C1, the GITT test is a cyclic process of pulse-constant current-relaxation, where pulse refers to a short constant current pulse, and relaxation refers to the process that no current passage. The basic principle is that a constant current i is applied for charging or discharging per unit time t, after which the current is disconnected and the voltage changes during the constant current process and the relaxation process are recorded simultaneously.[3]

The detailed calculation of the Zn^{2+} diffusion coefficient (D_{Zn}^{2+}) is as follows:[4]

$$D_{Zn^{2+}} = \frac{4}{\pi\tau}\left(\frac{n_m V_m}{S}\right)^2\left(\frac{\Delta E_s}{\Delta E_t}\right)^2 \quad (2)$$

Here, τ is the current pulse time (s). n_m, V_m and S represent the number of moles (mol), molar volume of the electrode ($cm^3\ mol^{-1}$) and the electrode/electrolyte contact area (cm^2), respectively. *ΔEs* represents the steady-state voltage change caused by current pulse; *ΔEt* represents the voltage change during the constant current pulse, removing the *iR* rise.

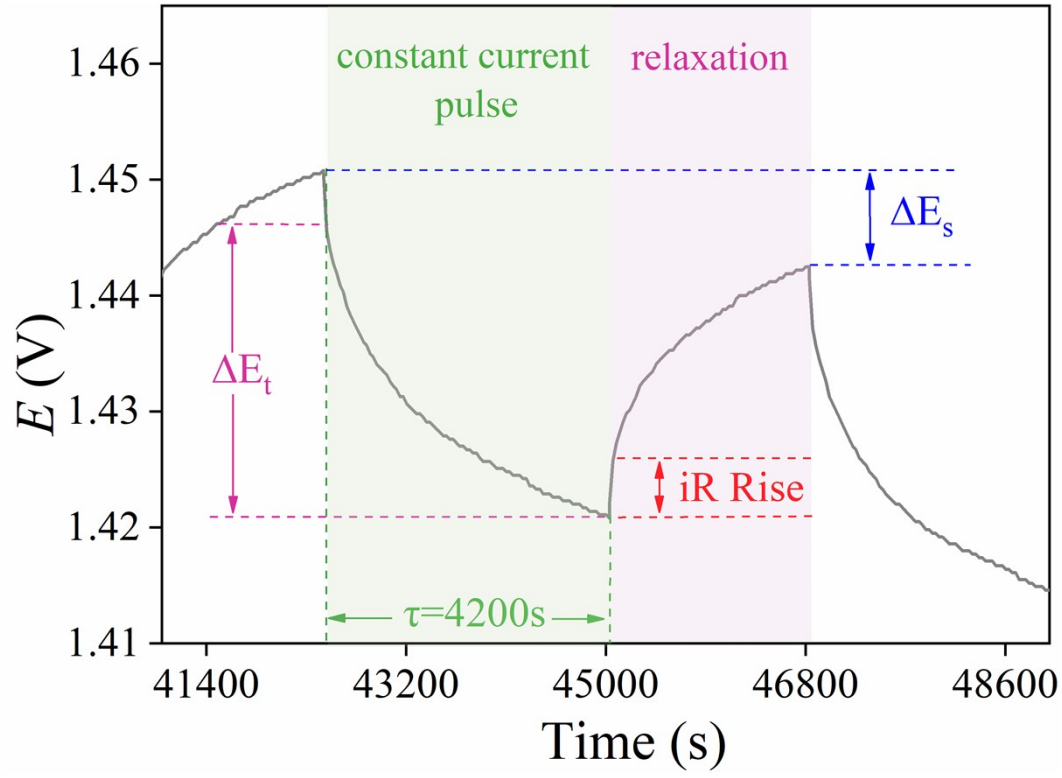

Fig. C1. Schematic diagram of a single charge step of GITT.

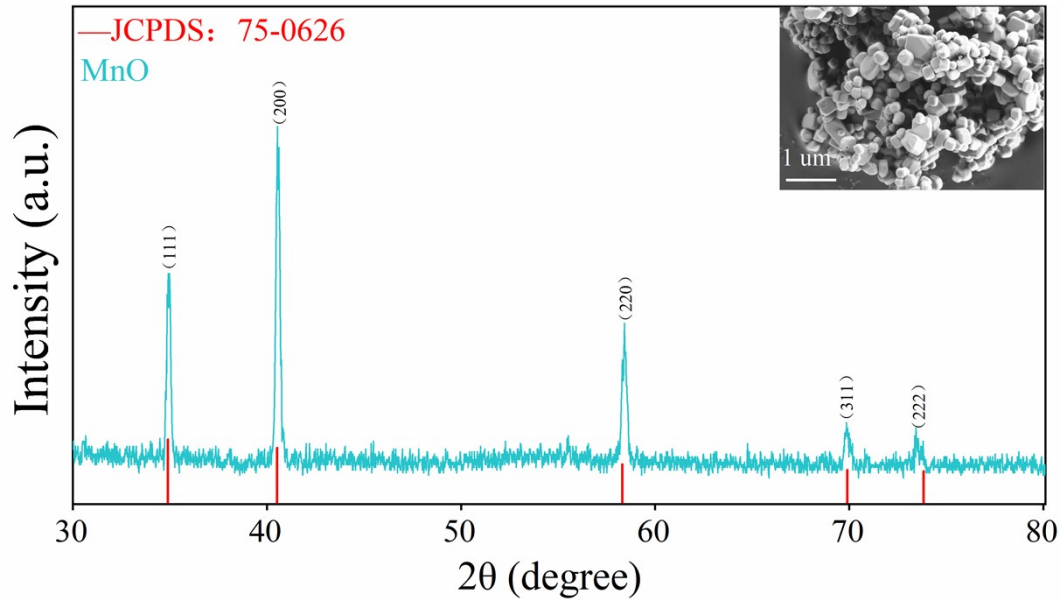

Fig. S1. XRD and SEM images of MnO synthesized by hydrothermal method.

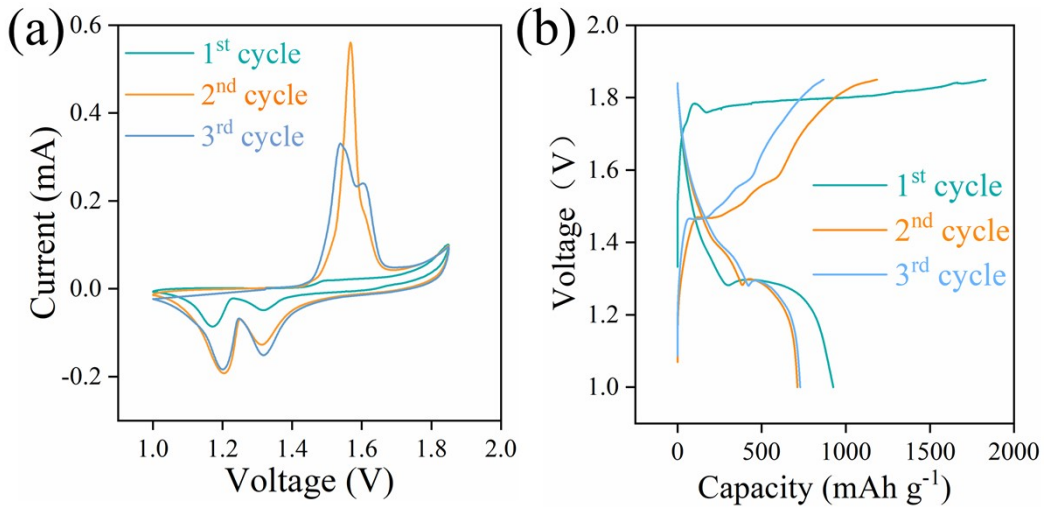

Fig. S2. (a) CV profiles of the 0.5 M $ZnSO_4$ + 0.5 M $MnSO_4$ system for the initial three cycles tested at a scan rate of 0.2 mV s^{-1}. (b) Charge/discharge profiles of the 0.5 M $ZnSO_4$ + 0.5 M $MnSO_4$ system for the first three cycles.

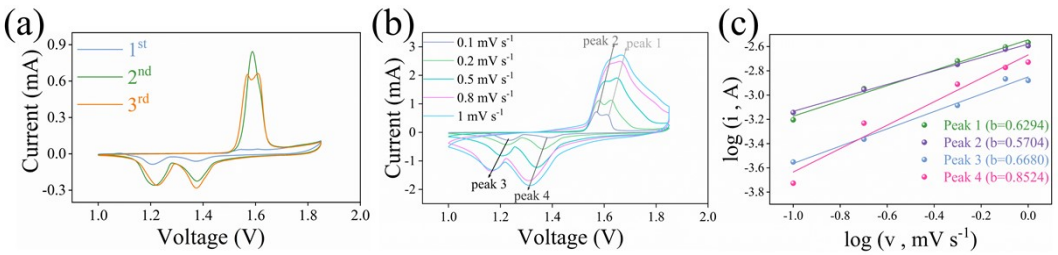

Fig. S3. (a) CV curves of the 2 M $ZnSO_4$ + 0.1 M $MnSO_4$ system for the first three cycles tested at a scan rate of 0.2 mV s^{-1}. (b) CV curves at multiple scan rates. (c) Log (i) *vs*. log (v) plots of four peaks in CV curves.

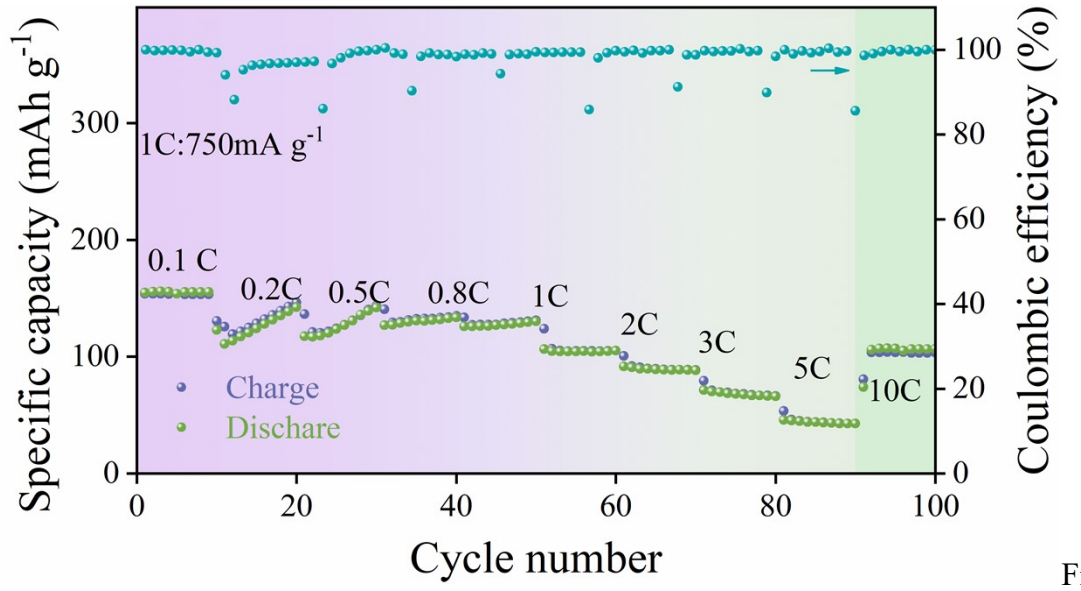

Fig. S4. Rate performance at 0.1-10 C of the cell with the 2 M $ZnSO_4$ + 0.1 M $MnSO_4$ (II) electrolyte.

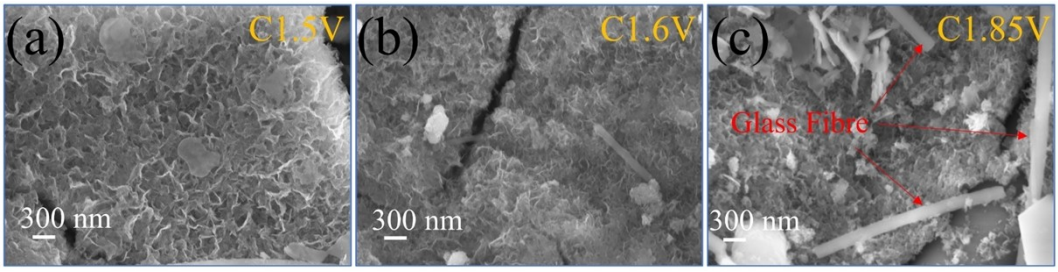

Fig. S5. Ex-situ SEM images of the cathode at different stages.

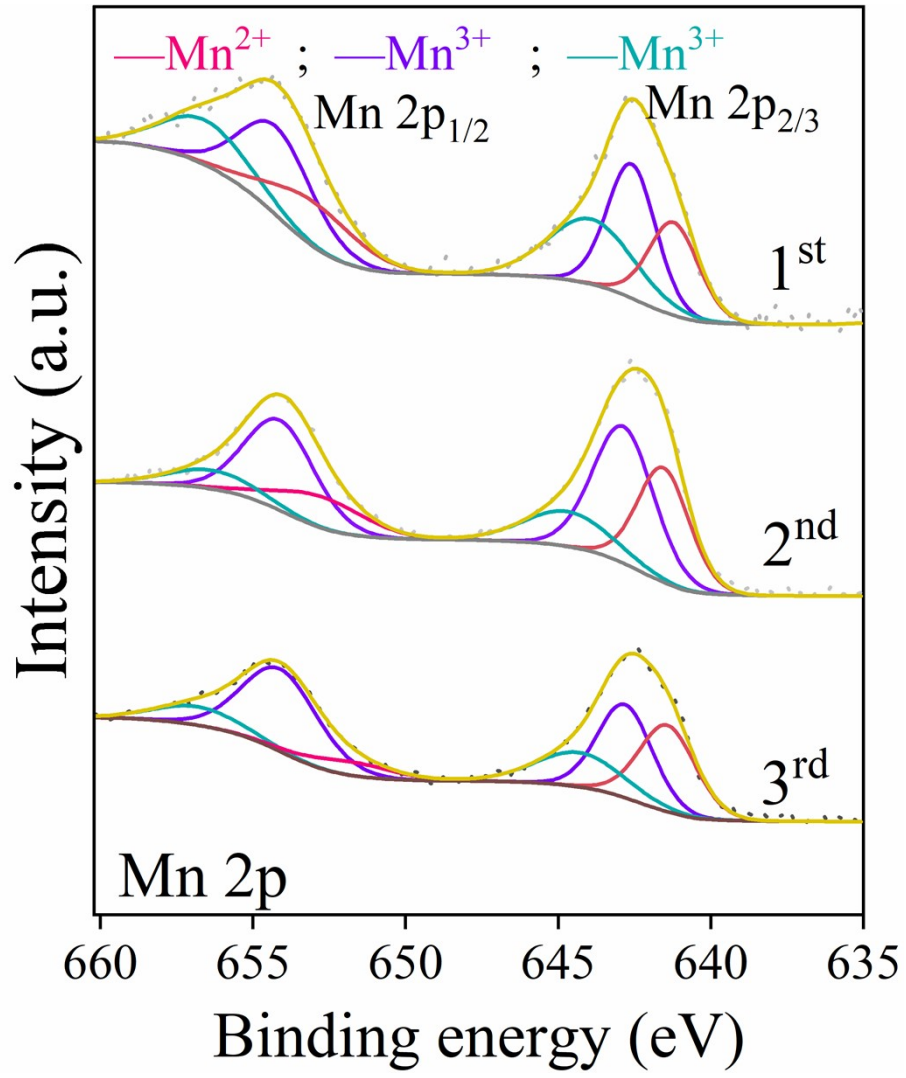

Fig. S6. High-resolution Mn 2p spectrum of the cathode after the first, second, and third charging process and its fitting result.

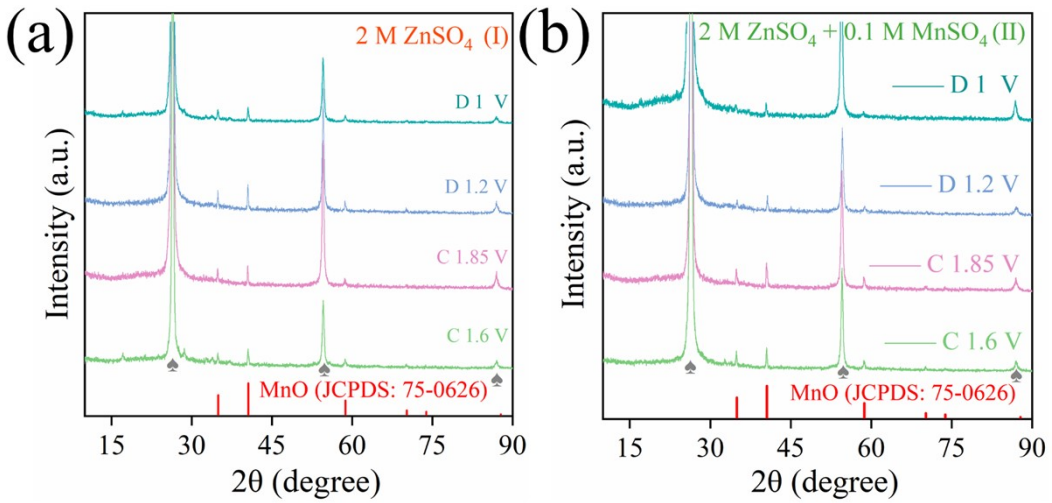

Fig. S7. Ex-situ XRD characterizations of cathodes from (a) 2 M $ZnSO_4$ (I) electrolyte, and (b) 2 M $ZnSO_4$ + 0.1 M $MnSO_4$ (II) electrolyte.

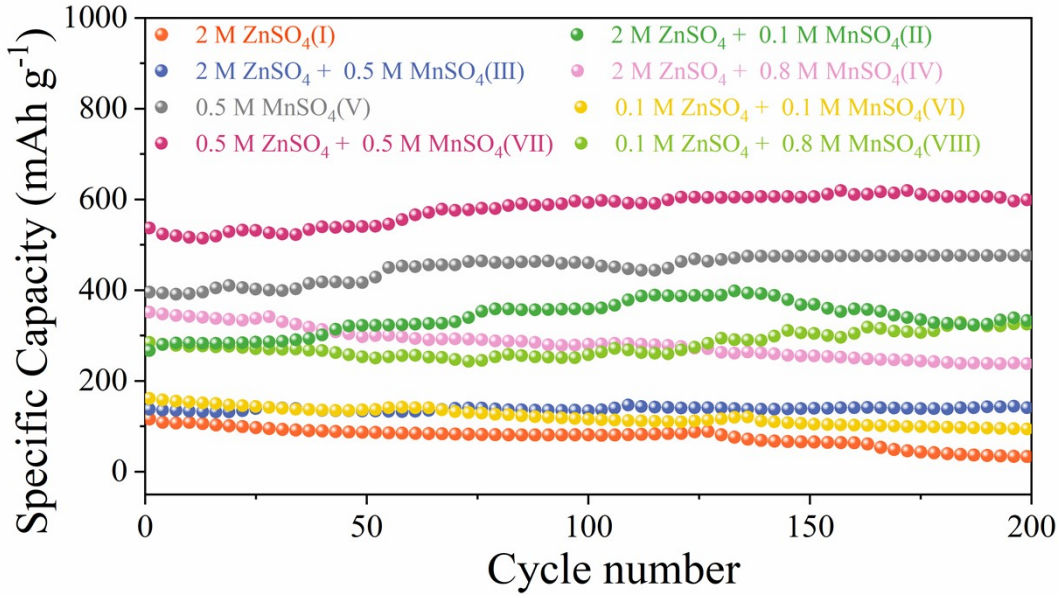

Fig. S8. Cycle performance for 200 cycles at 500 mA g^{-1}.

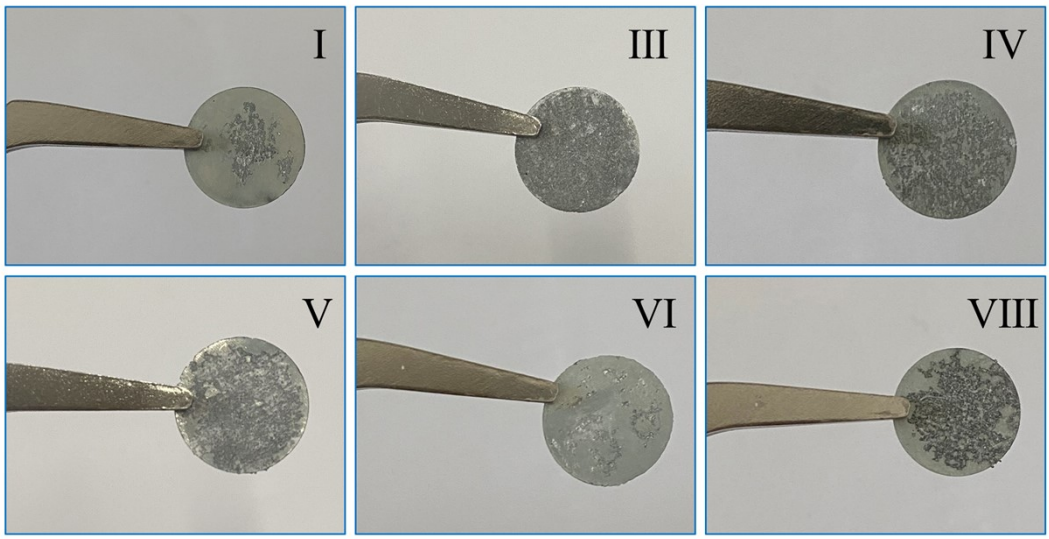

Fig. S9. Optical images of anode in different electrolytes after 200 cycles.

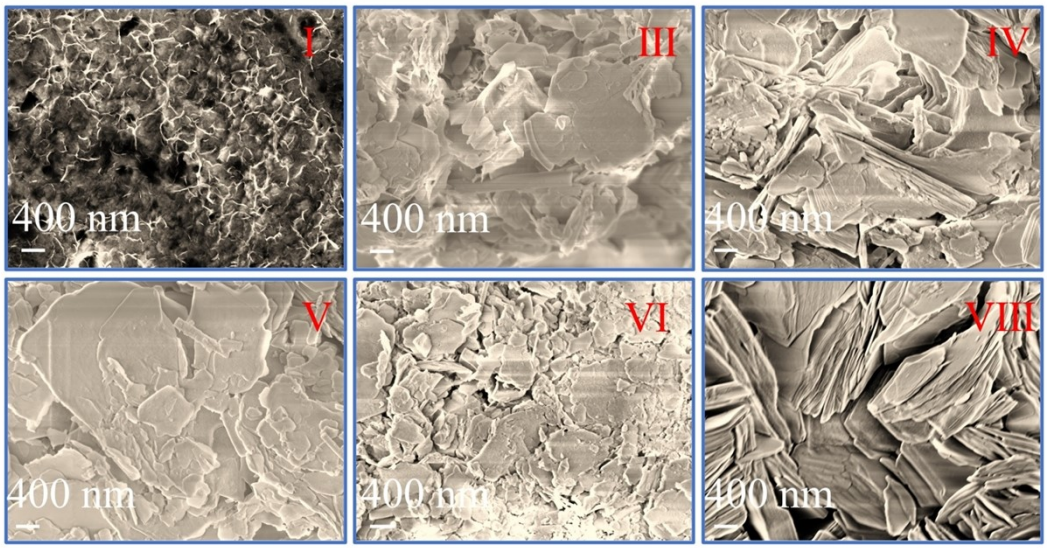

Fig. S10. SEM images of the anode in different electrolytes after 200 cycles.

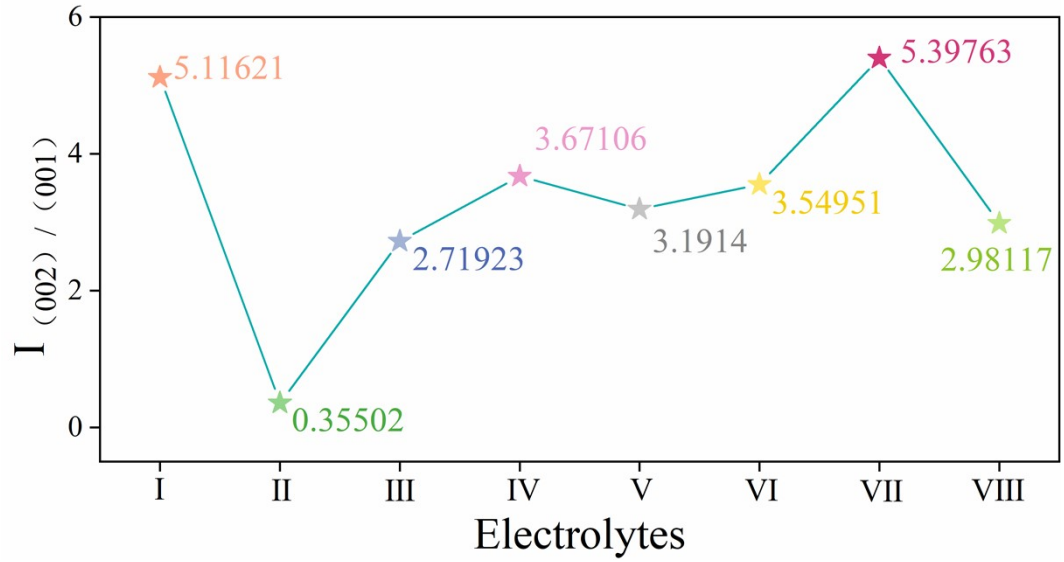

Fig. S11. The intensity ratio of (002)/(100) plane of zinc anodes from different electrolytes after 200 cycles according to the XRD results.

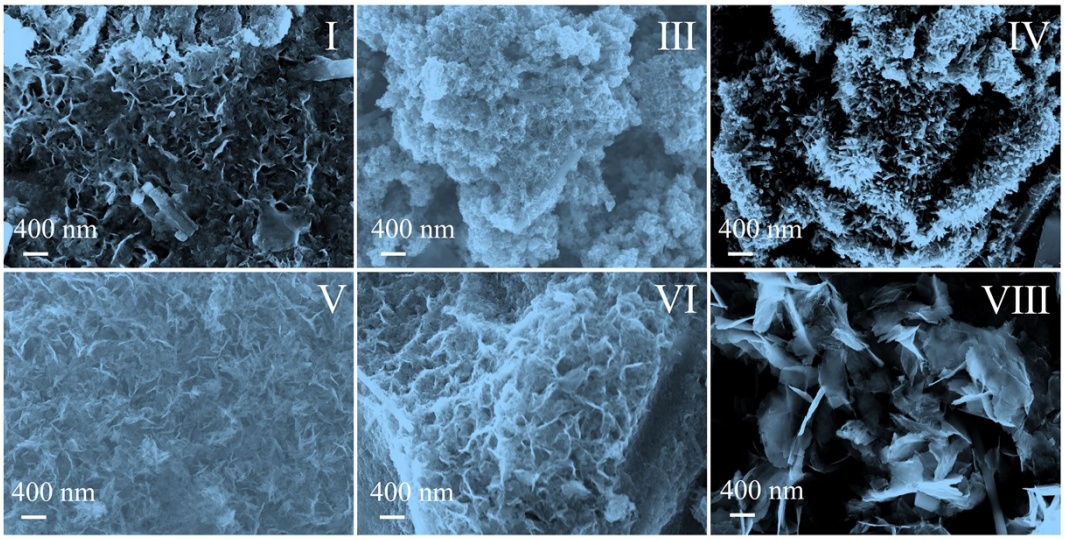

Fig. S12. SEM images of the cathode in different electrolytes after 200 cycles.

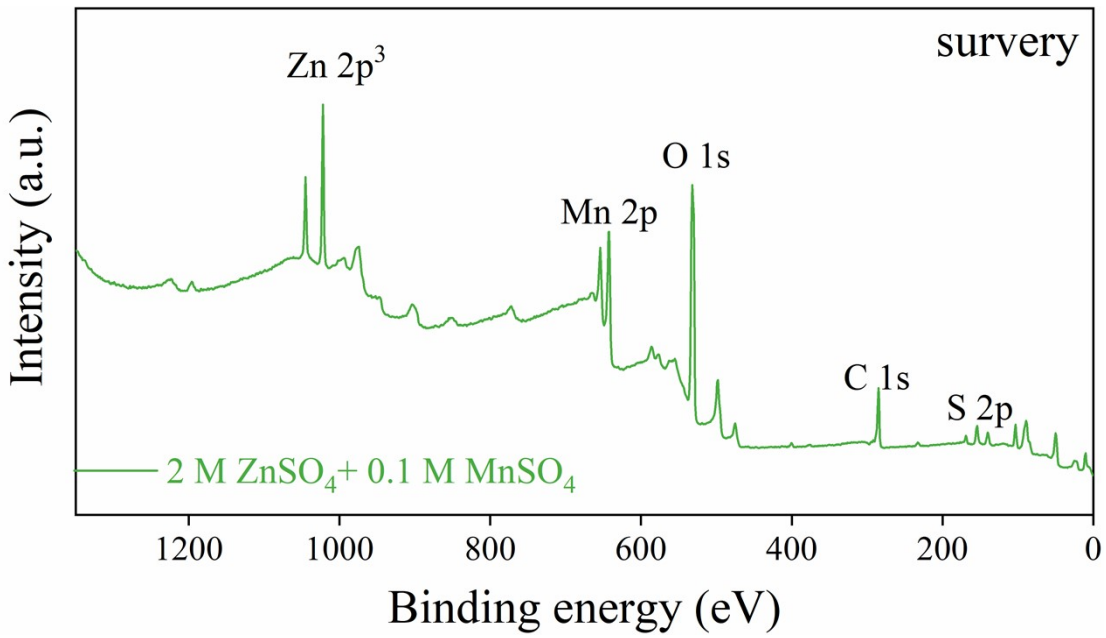

Fig. S13. XPS survey scan spectrum of the cathode in 2 M $ZnSO_4$ + 0.1 M $MnSO_4$ (II) electrolyte after 200 cycles.

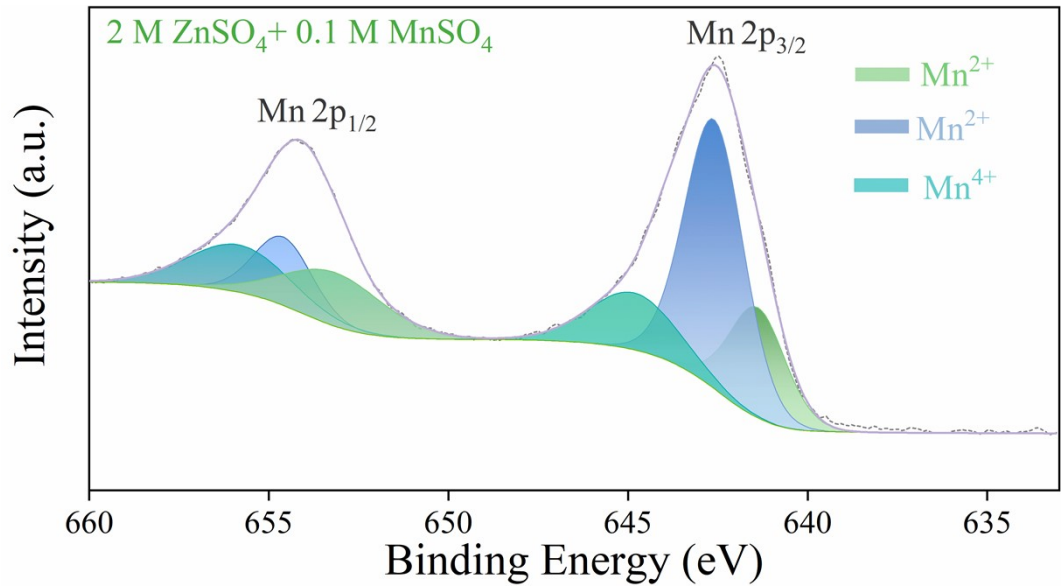

Fig. S14. High-resolution Mn 2p spectrum of the cathode in 2 M $ZnSO_4$ + 0.1 M $MnSO_4$ (II) electrolyte after 200 cycles.

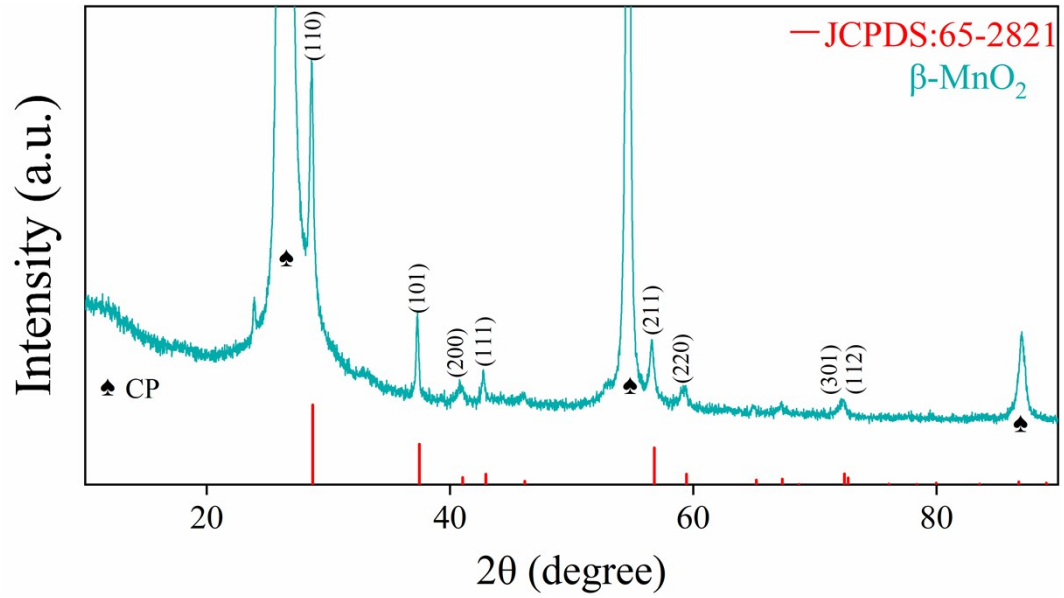

Fig. S15. XRD pattern of the as-prepared β-MnO_2 electrode.

Table S1. Comparison of electrochemical properties of ZIBs assembled with different electrolytes.

Electrolyte	Cycle number	Final Capacity (mAh g^{-1})	Rate performance (C)	Capacity Retention (%)	Coulombic Efficiency (%)
2 M $ZnSO_4$	1360	78	3	39	95.6
2 M $ZnSO_4$ + 0.1 M $MnSO_4$	850	110	3	52.4	99.7
2 M $ZnSO_4$ + 0.5 M $MnSO_4$	2000	54	7	55.1	99.8
2 M $ZnSO_4$ + 0.8 M $MnSO_4$	1300	29	5	85.3	99.1
0.5 M $MnSO_4$	1750	6	3	75	95.8
0.1 M $ZnSO_4$ + 0.1 M $MnSO_4$	2000	35	3	35	97.3
0.5 M $ZnSO_4$ + 0.5 M $MnSO_4$	5000	185	6	80	100
0.1 M $ZnSO_4$ + 0.8 M $MnSO_4$	1430	22	3	10	99.2

Table S2. Rs, Rsf and Rct values obtained by fitting EIS curves tested at different cycles.

Electrolyte		Initial Ω	5 Cycles Ω	30 Cycles Ω	100 Cycles Ω
2 M $ZnSO_4$	Rs	1.43	2.07	1.71	1.76
	Rsf	8.55	4.08	19.79	80.70
	Rct	425.40	3.87	629.40	760.20
2 M $ZnSO_4$ + 0.1 M $MnSO_4$	Rs	1.52	1.94	2.48	2.068
	Rsf	9.44	3.06	13.55	16.73
	Rct	346.00	35.87	452.10	749.1
2 M $ZnSO_4$ + 0.5 M $MnSO_4$	Rs	1.80	1.83	2.69	2.449
	Rsf	16.34	45.47	3.67	64.84
	Rct	644.60	224.10	303.70	959.4
2 M $ZnSO_4$ + 0.8 M $MnSO_4$	Rs	1.69	1.86	2.27	2.628
	Rsf	26.84	47.10	25.31	9.826
	Rct	558.60	7.398	292	534.1
0.5 M $MnSO_4$	Rs	2.08	9.34	6.76	8.28
	Rsf	4.17	5.51	103.30	63.10
	Rct	428.10	89.71	619.40	648.00
0.1 M $ZnSO_4$ + 0.1 M $MnSO_4$	Rs	3.21	4.92	4.23	5.45
	Rsf	19.79	18.33	121.50	97.40
	Rct	480.80	115.90	437.50	876.54
0.5 M $ZnSO_4$ + 0.5 M $MnSO_4$	Rs	1.54	2.85	2.85	3.13
	Rsf	7.11	4.94	34.39	19.11
	Rct	532.50	140.90	192.90	283.50
0.1 M $ZnSO_4$ + 0.8 M $MnSO_4$	Rs	1.54	6.43	6.86	5.691
	Rsf	6.58	4.20	58.32	136.2
	Rct	493.30	96.06	290.10	445.2

Table S3. Electrochemical performance of AZIBs with MnO cathode in different electrolytes.

Electrode Materials	electrolytes	Current density	Cycle number/ Discharge specific capacity	Reference
MnO@C	3 M $ZnSO_4$	2 A g^{-1}	10000/50 mAh g^{-1}	[5]
MnO	2 M $ZnSO_4$ + 0.2 M $MnSO_4$	1 A g^{-1}	1000/135 mAh g^{-1}	[6]
MnO-C	3 M $(CF_3O_3S)_2Zn$	0.1 A g^{-1}	40/727.7 mAh g^{-1}	[7]
MnO	2 M ZnSO4	1 A g^{-1}	1000/80 mAh g^{-1}	[8]
Cu-MnO	2 M $ZnSO_4$ + 0.1 M $MnSO_4$	3 C	1000/100 mAh g^{-1}	[9]
MnO@NGS	2 M $ZnSO_4$ + 0.2 M $MnSO_4$	0.5 A g^{-1}	300/100 mAh g^{-1}	[10]
MnO	2 M $ZnSO_4$	1 A g^{-1}	1500/116.4 mAh g^{-1}	[11]
55 wt% MnO with Bi_2O_3 and Cu	25 % KOH	0.19 A g^{-1}	350/600 mAh g^{-1}	[12]
MnO/MZ	3 M $ZnSO_4$	2 A g^{-1}	11000/50 mAh g^{-1}	[13]
MnO	0.5 M $ZnSO_4$ + 0.5 M $MnSO_4$	1 A g^{-1}	5000/248 mAh g^{-1}	Our work

References

1 W. Jiang, H. Shi, X. Xu, J. Shen, Z. Xu and R. Hu, *Energy Envion. Mater.*, 2021, **4**, 603-610.

2 H. Chen, J. Huang, S. Tian, L. Liu, T. Qin, L. Song, Y. Liu, Y. Zhang, X. Wu, S. Lei and S. Peng, *Adv Sci (Weinh)*, 2021, **8**, e2004924.

3 A. Nickol, T. Schied, C. Heubner, M. Schneider, A. Michaelis, M. Bobeth, G. Cuniberti, *J. Electrochem. Soc*., 2020, **167**, 090546.

4 T. He, S. Weng, Y. Ye, J. Cheng, X. Wang, X. Wang, B. Wang, *Energy Storage Mater.*, 2021, **38**, 389-396.

5 S. Li, D. Yu, L. Liu, S. Yao, X. Wang, X. Jin, D. Zhang, F. Du, *Chem. Eng. J*., 2022, **403**, 132673.

6 B. Yang, X. Cao, S. Wang, N. Wang, C. Sun, *Electrochim. Acta*, 2021, 385, 138447.

7 L. Cheng, J. Chen, Y. Yan, J. Zhang, H. Hu, J. Zhang, Y. Luo, Y. Chen, G. Wang, R. Wang, *Chem. Phys. Lett*., 2021, **778**, 138772.

8 Z. You, H. Liu, J. Wang, L. Ren, J.-G. Wang, *Appl. Surf. Sci*., 2020, **514**, 145949.

9 F.W. Fenta, B.W. Olbasa, M.-C. Tsai, M.A. Weret, T.A. Zegeye, *J.Mater. Chem. A*, 2020, **8**, 17595-17607.

10 W. Li, X. Gao, Z. Chen, R. Guo, G. Zou, H. Hou, W. Deng, X. Ji, J. Zhao, *Chem. Eng. J.*, 2020, **402**, 125509.

11 C. Zhu, G. Fang, S. Liang, Z. Chen, Z. Wang, J. Ma, H. Wang, B. Tang, X. Zheng, J. Zhou, *Energy Storage Mater*., 2020, **24**, 394-401.

12 G.G. Yadav, J. Cho, D. Turney, B. Hawkins, X. Wei, J. Huang, S. Banerjee, M. Nyce, *Adv. Energy Mater*., 2019, **9**, 1902270.

13 Y. Liu, Z. Qin, X. Yang, X. Sun, Adv. Funct. Mate., 2022, **32**, 2106994.